JOURNAL OF CATALYSIS 148, 729–736 (1994)

Pt–CeO_2 Contact and Its Effect on CO Hydrogenation Selectivity

D. S. Kalakkad,* A. K. Datye,*,[1] and H. J. Robota†

*Department of Chemical and Nuclear Engineering, University of New Mexico, Albuquerque, New Mexico 87131; and †Allied Signal Engineering Materials Research Center, Des Plaines, Illinois 60621

Received October 12, 1993; revised March 23, 1994

The CO_2/CH_4 ratio during methanation on Pt was found to be very sensitive to the proximity of Pt and CeO_2. On 0.6 wt% Pt/Al_2O_3, the CO_2/CH_4 ratio was ≈0.09 suggesting that most of the O from the CO ends up as H_2O in the product stream. In contrast, on 0.6 wt% Pt/CeO_2 the CO_2/CH_4 ratio ranged from 0.8–1.0. The selectivity to CO_2 was not a result of the sequential water-gas shift reaction nor was it caused by a surface reduction of CeO_2 by CO. The highest selectivity to CO_2 is observed on catalysts with the smallest Pt particle sizes, providing further evidence that Pt–CeO_2 contact influences the selectivity toward CO_2 formation. In this study, we have also investigated whether the CO_2/CH_4 ratio could be used as a probe of Pt–CeO_2 contact in Pt/CeO_2–Al_2O_3 catalysts. © 1994 Academic Press, Inc.

INTRODUCTION

CeO_2 is a very important additive in present day automotive exhaust catalysts. Addition of CeO_2 to these catalysts has been reported to provide oxygen storage (1), to promote the low temperature water-gas shift reaction (2), to minimize the thermally induced sintering of the alumina support (2), and to stabilize the noble metal dispersion (3). Previous work in our laboratory (4) also demonstrated that the addition of CeO_2 increases the CO hydrogenation activity of Pt/Al_2O_3, which is otherwise a poor catalyst for methanation. The promotion of methanation activity was observed regardless of the pretreatment of the catalyst, whether preoxidized or high temperature reduced (HTR). The extent of activity promotion was similar to that seen by Blankenburg *et al.* (5) when Pt was supported on titania. Likewise, when the Pt/CeO_2 catalyst was subjected to HTR, an effect similar to the classic SMSI (6) was seen, where the alkane hydrogenolysis activity dropped by over an order of magnitude compared to that in the preoxidized state. High resolution TEM, however, did not show any overlayers covering the Pt surface, in contrast to TiO_2-supported catalysts (7).

We also noticed a significant difference in product selectivity during CO hydrogenation on Pt/CeO_2 (8). The main products formed over these catalysts during CO hydrogenation were CH_4 and CO_2. The CO_2/CH_4 product ratio for these catalysts appeared to increase with increasing CeO_2 content. On Pt/Al_2O_3, the ratio was ≈0.1, on Pt/CeO_2–Al_2O_3 it was 0.7, while on Pt/CeO_2 it ranged between 0.8 and 1.0. When CO hydrogenation was performed immediately after the Pt/CeO_2 catalyst was oxidized, the CO_2/CH_4 ratio could be as high as 2.0 for the first few runs and then the ratio would level off to a steady state value between 0.8 and 1.0.

The enhanced CO_2/CH_4 ratio could result from a reduction of the CeO_2 surface by CO or from lattice oxygen provided by the CeO_2 (9). Another possibility is that the increased selectivity to CO_2 could be a result of a sequential water-gas shift occurring on the CeO_2 or on Pt/CeO_2 interfacial sites. As we show in this paper, we can rule out water-gas shift catalysis occurring in series as being responsible for the selectivity to CO_2. Furthermore, the enhanced CO_2/CH_4 ratio was seen during steady state catalysis, and even after high temperature reduction, leading us to believe that oxygen supplied by the ceria could not be causing the enhanced CO_2/CH_4 ratios during methanation. We conclude that there is a good correlation between Pt–CeO_2 contact and the CO_2/CH_4 ratio during methanation, and we have explored the possibility of using this CO_2/CH_4 ratio as a probe for Pt–CeO_2 contact in Pt/CeO_2–Al_2O_3 catalysts.

EXPERIMENTAL

A detailed description of the experimental setup has been given elsewhere (10). The catalyst powder was held between two quartz wool plugs in a ¼-in. o.d. quartz U-tube. Temperature was measured by a thermocouple inserted into the catalyst bed. For most runs approximately 50 mg of powder was used. CO hydrogenation reactions were carried out with an H_2 : CO ratio of 15 : 5 sccm (standard cubic centimeters per minute). The H_2 was research purity grade from Big Three and was 99.999% pure. Research purity CO from Matheson was further purified by passing through a bed of glass beads heated to 673 K to

---

[1] To whom correspondence should be addressed.

0021-9517/94 $6.00

decompose any carbonyls and through an ascarite trap to remove CO_2. The reactants were allowed to flow for 10 min over the catalyst in order to achieve steady state before sampling the effluent. Between successive runs, 15 sccm of H_2 was allowed to flow over the catalyst in order to regenerate the catalyst by removing any carbon that may have been deposited on the metal surface during the reaction. All temperature changes were made under flowing H_2. Water-gas shift reactions were performed with a stream of 15 sccm He and 5 sccm CO bubbled through a saturator filled with water at room temperature. *n*-butane hydrogenolysis was performed with a reactant stream containing H_2, He, and *n*-butane in the ratio 20 : 20 : 1 sccm.

Analysis was performed by gas chromatography on a Haysep N column and quantified by a flame ionization detector (FID). Since the FID is not sensitive to CO or CO_2, we used a methanizer to convert both of these products to CH_4. The products were first separated by the gas chromatograph column before being sent into the methanizer. H_2O cannot be detected with an FID but can be observed when a thermal conductivity detector is used for analysis. However, the broad, tailing peaks make the quantification of H_2O difficult and hence the only peaks quantified during a typical run were CO, CH_4, and CO_2. No higher molecular weight hydrocarbons were detected.

Table 1 shows the details of the catalysts used in this study. The catalysts marked [a] were prepared by impregnating the support with chloroplatinic acid (H_2PtCl_6), dried in air, and then calcined at 600°C. The catalysts marked [b] were made by impregnating the CeO_2 support with $PtCl_4$, dried in air at 110°C, and then calcined at 500°C. The Pt/Al_2O_3, Pt/CeO_2–Al_2O_3, and the Pt/CeO_2 (0.6 wt%) were the catalysts that were used in our previous study of the interaction between Pt and CeO_2 in automotive exhaust catalysts (10). Before the reactions were performed, all catalysts were reduced at 400°C, and this is termed the fresh state of the catalyst. The preoxidized state of the catalyst refers to an oxidation pretreatment in flowing 10% O_2 in He at 500°C, and the high temperature reduction (HTR) refers to a reduction pretreatment in flowing H_2 at 500°C.

Transmission electron microscopy was used to assess the particle sizes in these catalysts. TEM was done using a JEOL JEM 2000 FX 200 kV electron microscope at the University of New Mexico. The samples for TEM were prepared by simply dipping carbon coated copper grids in the powder sample and shaking off the excess. No solvents were used during any stage of the sample preparation.

RESULTS

Transmission Electron Microscopy

Figure 1 shows the TEM micrograph for a 0.1 wt% Pt/CeO_2 sample whose average particle size is 14 Å. It can be seen that the particles are fairly well dispersed throughout the CeO_2 support. Figure 2 shows the TEM micrograph of a 1.0 wt% Pt/CeO_2 catalyst. The average particle size has increased over that in the 0.1% catalyst. The average particle size in this catalyst is approximately 24 Å. The overall distribution in this catalyst is less uniform than in the 0.1 wt% catalyst and particles as large as ≈70 Å were seen in the catalyst. Figure 3 shows the micrograph for the 10 wt% Pt/CeO_2 catalyst. The average particle size has further increased in this catalyst and the overall nonuniformity of the particle size is much more

TABLE 1

Catalysts Used in This Study

Catalyst	Precursor	Support	Surface area of support	Wt loading Pt
Pt/Al_2O_3[a]	H_2PtCl_6	Degussa AlonC (γ + δ alumina)	≈100 m^2/g	0.6 wt%
Pt/CeO_2–Al_2O_3[a]	H_2PtCl_6	12 wt% ceria on Degussa AlonC	≈100 m^2/g	0.6 wt%
Pt/CeO_2[a]	H_2PtCl_6	CeO_2 precipitated from $Ce(NO_3)_3$	≈7.0 m^2/g	0.6 wt%
Pt/CeO_2[b]	$PtCl_4$	CeO_2 precipitated from $Ce(NO_3)_3$	≈7.0 m^2/g	0.7 wt% 6.0 wt%
Pt/CeO_2[b]	$PtCl_4$	CeO_2 from Aldrich Chemicals	≈7.0 m^2/g	0.1 wt% 1.0 wt% 3.0 wt% 10. wt%

[a] See text.

[b] See text.

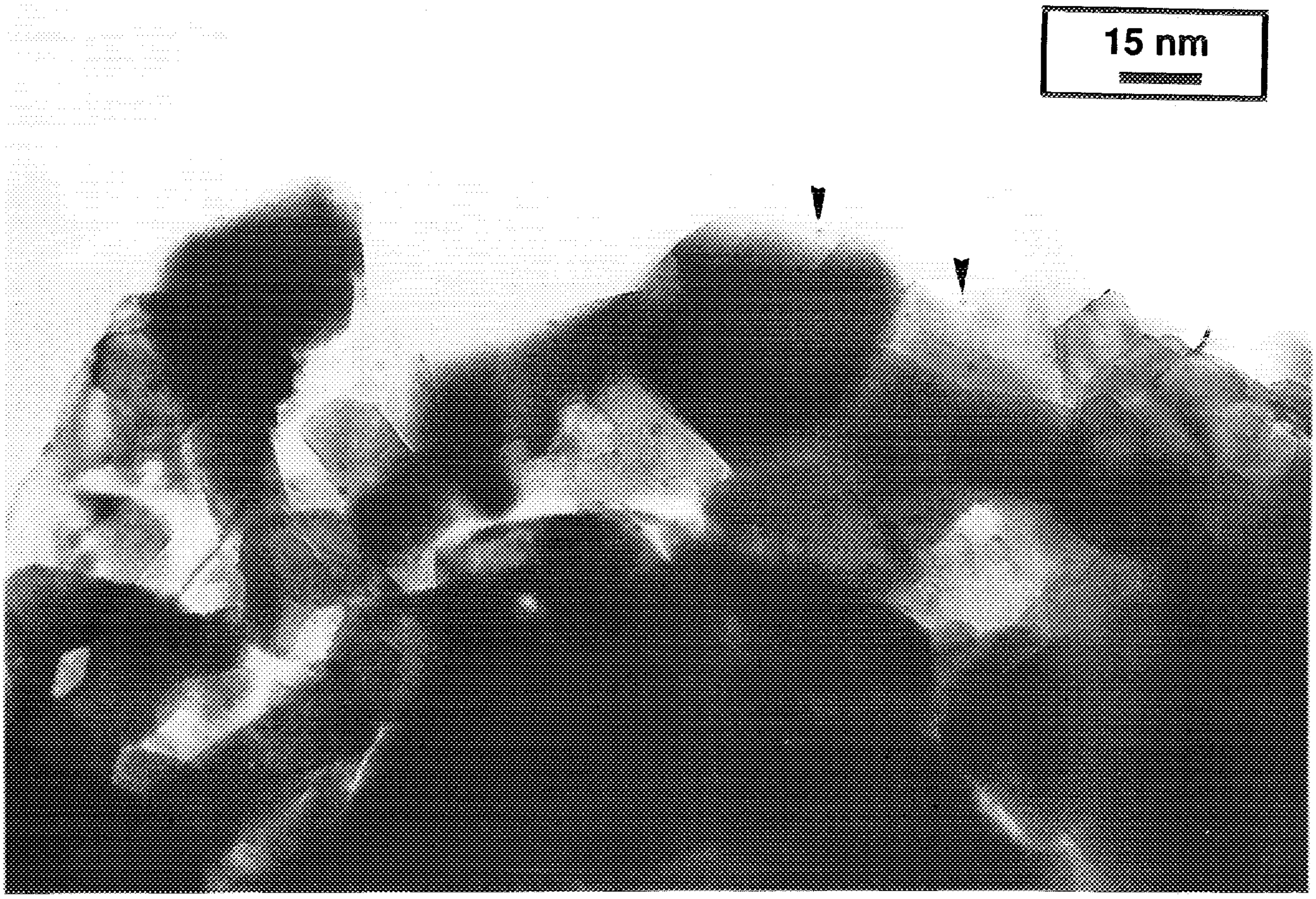

FIG. 1. TEM micrograph of 0.1 wt% Pt/CeO_2 catalyst. Arrows indicate Pt particles.

pronounced. The average particle size in this catalyst is ≈90 Å, but particles as large as 300 Å are seen frequently in this catalyst. These Pt/CeO_2 catalysts with weight loadings spanning two orders of magnitude provide us with samples having increased particle size with increasing Pt loading. For the sake of brevity, the TEM results on catalysts with intermediate compositions have not been included here.

Reactivity Studies

We first investigated whether the water-gas shift reaction proceeded to a significant extent under the experimental conditions used for methanation. Figure 4 shows a comparison of the WGS activity of these catalysts with the methanation activity. Our experimental conditions were chosen so that the partial pressure of H_2O during WGS was comparable to that during methanation. For example, the partial pressure of H_2O during water-gas shift was approximately 17.5 Torr (saturator temperature 293 K) with the ratio of $H_2O/CO \approx 0.12$. During CO hydrogenation, a water partial pressure of 17.5 Torr would be reached at a conversion of about 11%, at which point the H_2O/CO ratio would be 0.12. Therefore, the reactant partial pressures during the WGS and methanation are comparable, except for the presence of H_2 during the latter. From Fig. 4, it can be seen that the WGS activity is approximately an order of magnitude greater than that for methanation on all of these catalysts. This would mean that all three catalysts are capable of converting any water formed into CO_2.

Sequential WGS could occur via two mechanistic pathways, as shown below:

$$\begin{array}{l} CO + 3H_2 \xrightarrow{Pt} CH_4 + H_2O \\ H_2O + CO \xrightarrow{CeO_2} CO_2 + H_2 \end{array} \quad [1]$$

$$\frac{CO_2}{CH_4} = 1.0$$

$$\begin{array}{l} CO + 3H_2 \xrightarrow{Pt} CH_4 + H_2O \\ H_2O + CO \xrightarrow{Pt/CeO_2} CO_2 + H_2 \end{array} \quad [2]$$

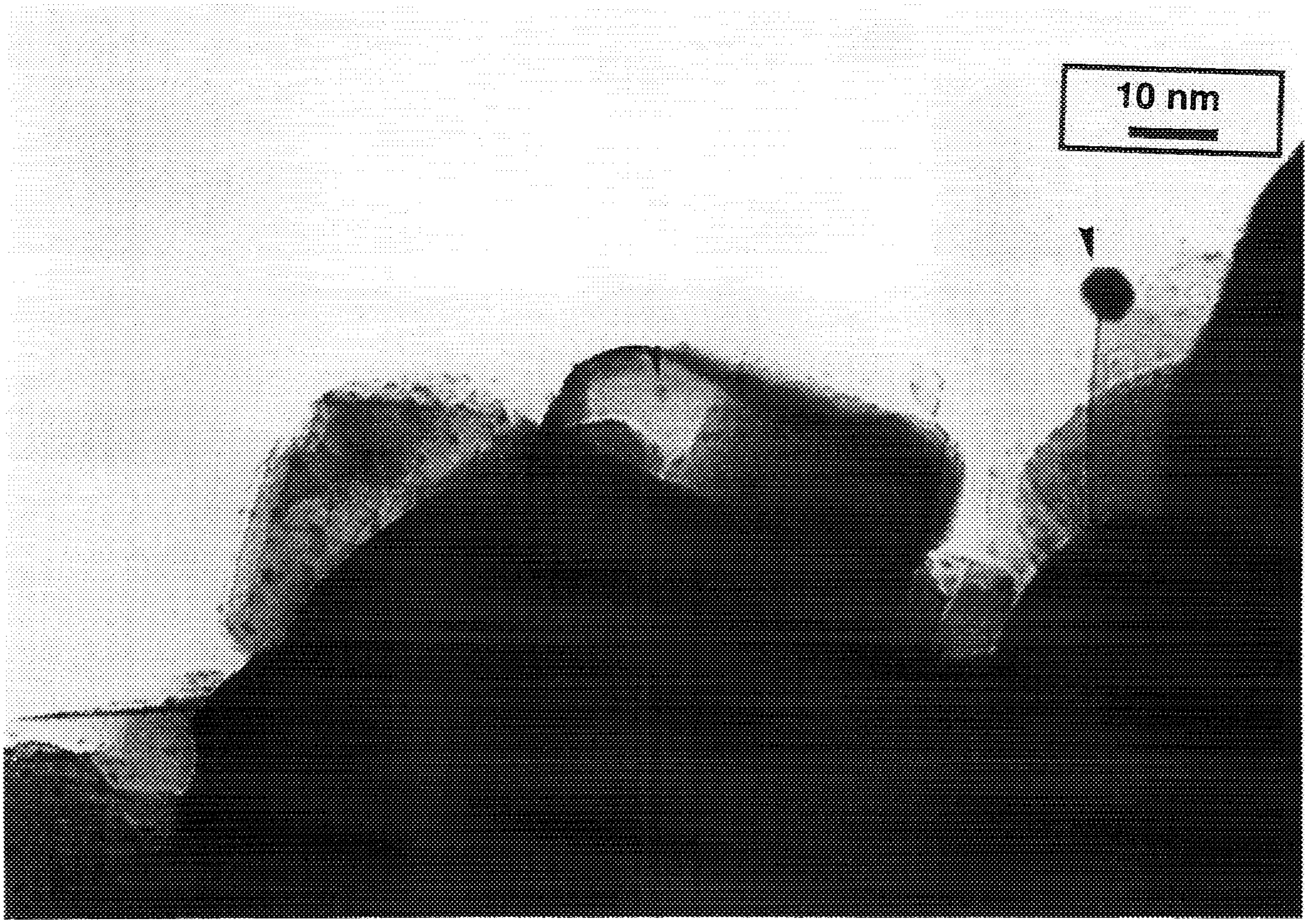

FIG. 2. TEM micrograph of 1.0 wt% Pt/CeO_2 catalyst. Arrows indicate Pt particles.

Our first experiment was to check if the water formed on Pt was converted to CO_2 by a sequential water-gas shift reaction on the CeO_2 support as shown in Eq. [1]. For this purpose, we had a small bed of Pt/Al_2O_3 followed by a long bed of CeO_2. If a sequential water-gas shift reaction was involved, the CO_2/CH_4 ratio seen on such an arrangement would have been grater than that seen on Pt/Al_2O_3. Table 2 shows the results of this experiment. We can see that the CO_2/CH_4 ratio is unaffected by the CeO_2 bed placed in series with the Pt/Al_2O_3 regardless of the pretreatment. This proves that the pathway in Eq. [1] can be ruled out.

We next examined the pathway shown above in Eq. [2], where the formation of CO_2 may occur via a water-gas shift on the Pt/CeO_2 itself. This would mean that the formation of CO_2 is through a series reaction of the form $A \rightarrow B \rightarrow C$, where A is CO, B is H_2O, and C is CO_2. For such a mechanism, we would expect the ratio C/B to increase with % conversion. Since we were unable to quantify B with our analytical setup, we monitored the CO_2/CH_4 ratio as a measure of the C/B. Figure 5 shows the CO_2/CH_4 ratio as a function of conversion on a Pt/CeO_2–Al_2O_3 catalyst over a range of conversions varying between ≈0.1 and 70%. Conversion was varied by varying the reaction temperature. It can be seen that the ratio did not vary significantly with conversion, contrary to what would be expected for a series reaction. Thus, it was inferred that the pathway shown in Eq. [2] was not responsible for the increased CO_2/CH_4 ratio on the CeO_2 containing catalysts.

TABLE 2

Results—Sequential Bed Pt/Al_2O_3 Followed by a Long Bed of Pure CeO_2

State of the catalyst	CO_2/CH_4
Fresh	0.16
Preoxidized (10% O_2, 773K)	0.14
HTR (H_2, 773 K)	0.17

Note. CO hydrogenation—$H_2:CO = 15:5$. Temperature = 623 K.

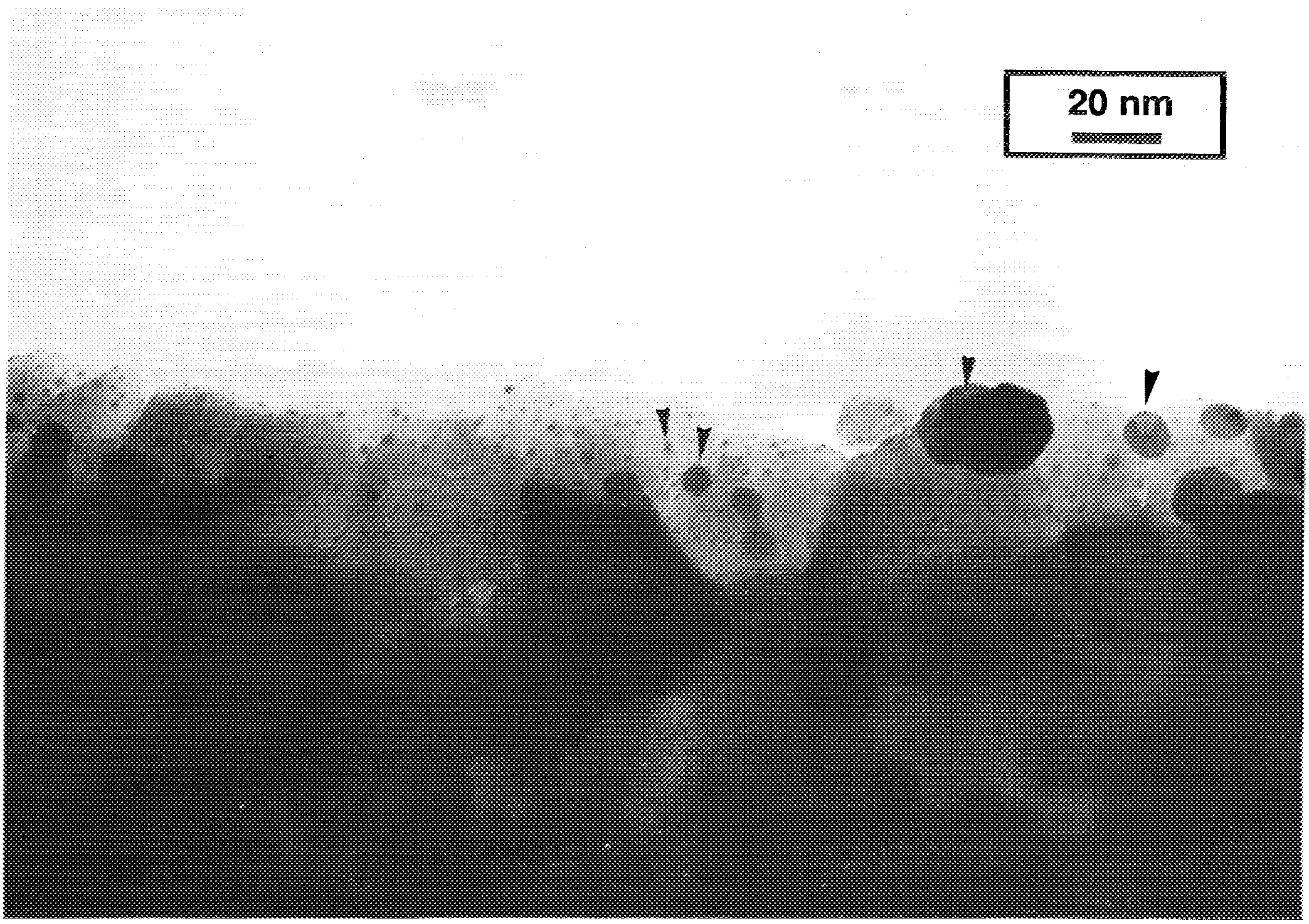

FIG. 3. TEM micrograph of 10.0 wt% Pt/CeO_2 catalyst. Arrows indicate Pt particles.

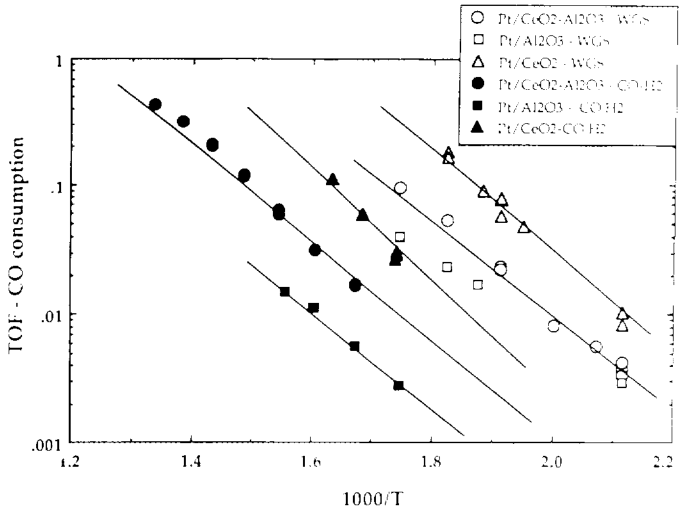

FIG. 4. Water-gas shift and methanation activities of Pt/Al_2O_3, Pt/CeO_2–Al_2O_3, and Pt/CeO_2. H_2 : CO for methanation, and He : CO for water-gas shift = 15 : 5. TOF CO consumption = CO consumed/surface Pt/s.

The inability to see any evidence for the water-gas shift reaction in series with the methanation reaction suggests that H_2O may be unable to adsorb on the catalyst in competition with the other reactants present during methanation. Furthermore, the WGS activity of Pt/CeO_2–Al_2O_3 was only a factor of 2 greater than that of Pt/Al_2O_3, which is not sufficient to account for the factor

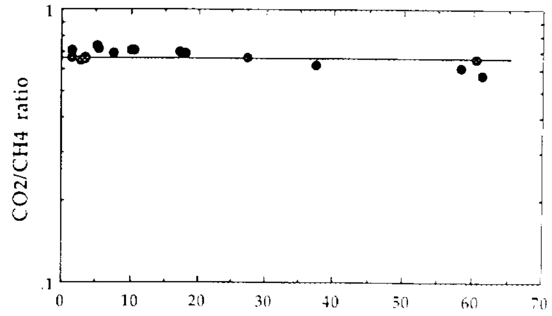

FIG. 5. CO_2/CH_4 ratio during methanation as a function of CO conversion on Pt/CeO_2–Al_2O_3. H_2 : CO = 15 : 5.

of 7 difference in the CO_2/CH_4 ratio. These experiments all suggest that sequential WGS was not responsible for the increase in the CO_2/CH_4 ratio observed on CeO_2 containing catalysts. It is therefore appropriate to conclude that the presence of CeO_2 in contact with Pt somehow modifies the selectivity during methanation leading to an increase in the CO_2/CH_4 ratio.

The nature of the Pt/CeO_2 contact necessary for the altered selectivity was also investigated. As described earlier, a long bed of CeO_2 in series with a bed of Pt/Al_2O_3 had no effect on the CO_2/CH_4 ratio. To increase the contact, we prepared a 1 : 1 physical mixture of Pt/Al_2O_3 and pure CeO_2 by grinding the two components thoroughly. Table 3 shows the CO_2/CH_4 ratio from this mixture after various pretreatments. In the fresh state, the CO_2/CH_4 ratio is similar to that on Pt/Al_2O_3, thus showing again that the presence of CeO_2 in close proximity to Pt does not result in an increase in the CO_2/CH_4 ratio. However, after the first high temperature pretreatment, we see a rise in the CO_2/CH_4 ratio, suggesting that contact has been established between Pt and CeO_2. At this stage we are unable to comment on how the Pt–CeO_2 contact is achieved, but it may involve a migration of Pt onto CeO_2 or vice versa (11). It is possible that a similar mechanism is at play in automotive catalysts, where it has been found that impregnation of ceria on an aged Pt/Al_2O_3 catalyst can lead to improvement in catalytic performance (12). If Pt–CeO_2 contact is indeed responsible for the altered CO_2/CH_4 ratio, we would expect this ratio to be affected by Pt particle size, which can be manipulated by varying the catalyst metal loading.

Figure 6 shows the variation in the CO_2/CH_4 ratio as a function of the % metal loading (by weight) on the series of Pt catalysts listed in Table 1. It was verified by TEM that the average particle size in these catalysts increased with increasing Pt loading. The CO_2/CH_4 ratio is seen to decrease as the weight loading of the catalyst increases, suggesting that smaller Pt particle sizes which provide increased metal–oxide interfacial area tend to favor the formation of CO_2 during methanation.

In previous work (8), we also observed an increase in methanation activity on Pt/CeO_2 compared to Pt/Al_2O_3. We expressed the enhancement in methanation in terms of the ratio of methanation to hydrogenolysis activities in the fresh state, where the SMSI effect does not suppress hydrogenolysis activity. Figure 7 shows the methanation/hydrogenolysis ratio for Pt/CeO_2 catalysts as a function of weight loading and also the data for the Pt/Al_2O_3 catalyst. The higher methanation activity on CeO_2-containing catalysts is immediately apparent. However, the relative activity (methanation/hydrogenolysis) appears to be unaffected by Pt particle size, indicating that the effect of Pt particle size is similar on both reactions. The literature suggests that specific hydrogenolysis activity increases with decreasing particle size, whereas the specific activity for methanation is rather insensitive to particle size (13). Based on this indirect evidence, we may conclude that metal–ceria contact in the smaller particles may be causing an increase in methanation activity. We have not attempted to directly quantify the effect of Pt–CeO_2 contact on methanation activity in view of potential uncertainties in chemisorption uptake (especially with low-weight-loaded catalysts).

TABLE 3

Results—1 : 1 Physical Mixture $Pt/Al_2O_3 : CeO_2$

State of the catalyst	CO_2/CH_4
Fresh	0.15
Preoxidized	0.5
HTR	0.65

Note. CO hydrogenation—H_2 : CO = 15 : 5. Temperature = 623 K.

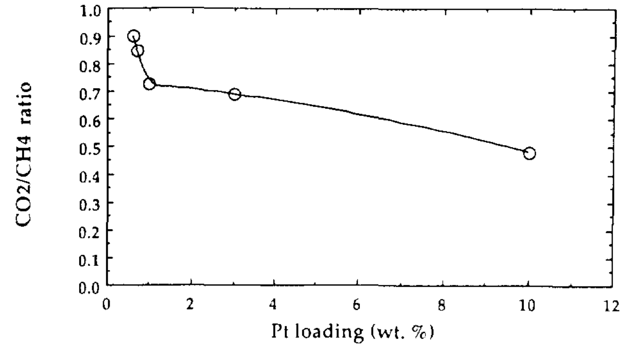

FIG. 6. CO_2/CH_4 ratio during methanation as a function of Pt weight loading on Pt/CeO_2 catalysts. H_2 : CO = 15 : 5.

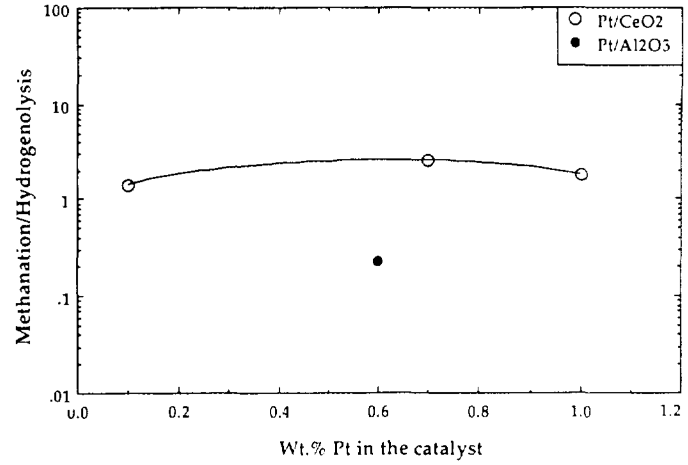

FIG. 7. Methanation/hydrogenolysis ratio on Pt/CeO_2 catalysts as a function of Pt weight loading. Also shown is the data for Pt/Al_2O_3.

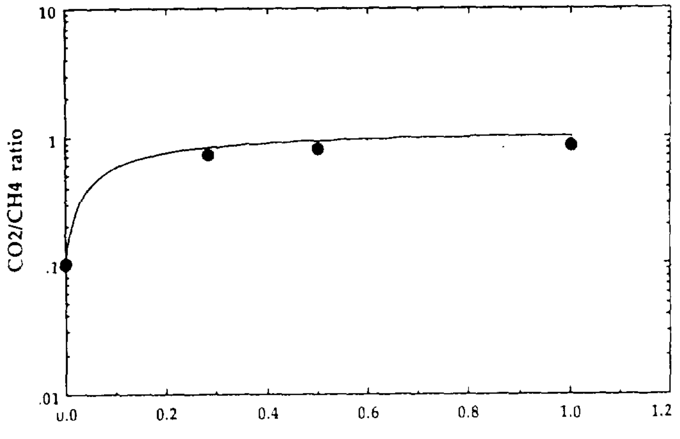

FIG. 8. CO_2/CH_4 ratio during methanation as a function of % Pt in contact with CeO_2 varied by preparing physical mixtures of Pt/CeO_2 and Pt/Al_2O_3. H_2 : CO = 15 : 5.

Since we wanted to use the CO_2/CH_4 ratio to infer the extent of Pt–CeO_2 contact in automotive catalysts, we prepared physical mixtures of Pt/Al_2O_3 and Pt/CeO_2 as calibration standards to explore this concept. Figure 8 shows the data on CO_2/CH_4 ratios with increasing amounts of Pt/CeO_2 in these mixtures. The relationship is not linear due to the higher methanation activity of CeO_2-containing catalysts. In effect, the CO_2/CH_4 ratio of Pt/CeO_2 dominates the behavior of the physical mixture of Pt/Al_2O_3 and Pt/CeO_2. The smooth curve in Fig. 8 was calculated assuming that Pt/CeO_2 has a CO_2/CH_4 ratio of 1.0 and that the Pt/CeO_2 is 10 times as reactive as Pt/Al_2O_3 for methanation. The two experimental points fall very nicely on this curve within experimental limits.

DISCUSSION

Our results show that Pt/Al_2O_3 catalysts produce H_2O during methanation, whereas Pt/CeO_2 catalysts produce CO_2. The first possibility is that the water-gas shift reaction occurs on the Pt/CeO_2 catalyst and transforms any H_2O produced into CO_2. As seen from Fig. 4, the WGS activity of all of the catalysts we studied was over an order of magnitude greater than their methanation activity. Therefore, we would expect any H_2O that is formed during methanation to be converted to CO_2. Since we see very little CO_2 on Pt/Al_2O_3 during methanation, we can conclude that the WGS reaction does not proceed to a significant extent during methanation. It is possible that excess H_2 present during methanation inhibits the readsorption of H_2O. All of our experiments confirmed the absence of any sequential WGS under methanation reaction conditions. For example, a postreaction bed of CeO_2 had no effect on the CO_2/CH_4 ratio, nor was there any effect of conversion such as would be expected for a series reaction.

The second possibility is that the excess CO_2 comes from a reduction of the CeO_2 surface or via lattice oxygen supplied by the CeO_2. Jin *et al.* (9) showed that significant conversions of CO to CO_2 occurred when CO adsorbed on Pt/CeO_2 was desorbed by heating the catalyst during temperature programmed desorption (TPD). They proposed that CO adsorbed on Pt could react with lattice oxygen on CeO_2 to form CO_2. The pool of lattice oxygen that led to CO_2 formation was approximately six times as large as the number of CO atoms on the Pt surface. However, the availability of lattice oxygen was greatly affected by pretreatment. Reduction at 773 K with H_2 completely suppressed the formation of CO_2, implying that the pool of lattice oxygen was depleted by this treatment. Exposure to oxygen at 373 K could replenish this pool of lattice oxygen. Heating the catalyst to 800 K also replenished this interfacial oxygen, presumably by oxygen from the bulk of the ceria lattice. Our experiments were performed under a reducing atmosphere with a 3 : 1 ratio of H_2/CO; we found no effect due to reduction in H_2 for over 48 h at 773 K, under which conditions we would be expected to rapidly deplete the supply of available lattice oxygen. Furthermore, we do not heat the catalyst between runs, which makes it unlikely that any interfacial oxygen that has reacted with the CO could be replenished by oxygen from the bulk of the ceria. Therefore, we conclude that it is unlikely that the increased CO_2 production we observe during methanation could be caused by lattice oxygen from the ceria.

Nunan *et al.* (14) have shown by TPR that surface reduction of ceria by H_2 can occur rapidly at temperatures as low as 493 K when CeO_2 is in contact with a noble metal like Pt. On the other hand, reduction of bulk ceria takes place at considerably higher temperatures, ≈773 K. The reaction temperatures during methanation are high enough for surface reduction of CeO_2 by CO. We would expect such a surface reduction to cause a transient in CO_2 production, and we have indeed observed an increase in CO_2/CH_4 ratios over their steady-state values immediately after the Pt/CeO_2 was subjected to preoxidation. However, this transient in CO_2 production subsided after two runs of 20 min duration at reaction temperature. Since the methanation reaction is carried out under reducing conditions, and the catalyst is exposed to flowing H_2 between runs, the surface reduction observed by Nunan *et al.* (14) should occur very rapidly. Therefore, it is unlikely that reduction of surface oxygen on ceria could cause the observed increase in CO_2/CH_4 ratios for steady-state catalysis.

It can therefore be ruled out that sequential water-gas shift or oxygen supplied by ceria may be responsible for the increase in CO_2/CH_4 ratio when Pt is supported on

CeO_2. We feel therefore that this increase is related to an intrinsic change in the catalytic sites on Pt/CeO_2. Yao and Yao (15) have shown that the presence of precious metal in close proximity to CeO_2 increases the oxygen storage capacity of CeO_2. Their studies indicate that the presence of a precious metal in contact with CeO_2 increases the extent of both removal and restoration of the oxygen anion by CO. This may give rise to a situation where an oxygen anion lost by one CO molecule in the process of methanation may be picked up by another CO molecule to give a CO_2/CH_4 ratio of 1.0. We feel that this may be a plausible mechanism to explain the increase in the CO_2/CH_4 ratio during methanation.

The correlation between CO_2/CH_4 ratio and Pt/CeO_2 contact suggests that this ratio could, in principle, be used to monitor the extent of Pt–CeO_2 interaction in automotive catalysts. However, since Pt–CeO_2 contact also leads to enhanced methanation activity, the CO_2/CH_4 ratio increases rapidly as small amounts of CeO_2 are introduced. In practice, large changes in Pt/CeO_2 contact cause very small changes in CO_2/CH_4 ratio. The nonlinear relationship between the CO_2/CH_4 ratio and the extent of Pt–CeO_2 contact would give rise to rather large error bars, making the method unreliable.

CONCLUSIONS

The CO_2/CH_4 product ratio during methanation was shown to be very strongly influenced by Pt–CeO_2 contact. Sequential water-gas shift reaction and surface reduction of ceria by CO were ruled out as being responsible for the observed increase in CO_2/CH_4 ratio in going from Pt/Al_2O_3 to Pt/CeO_2. Our results suggest that the selective formation of CO_2 as opposed to H_2O is a result of an intrinsic change in the mechanism when Pt is in contact with CeO_2. A physical mixture of Pt/Al_2O_3 with CeO_2 is not sufficient to bring about this increase in the CO_2/CH_4 ratio, implying that actual contact between Pt and CeO_2 is essential. However, it appears that high temperature cycling makes it possible to achieve metal–CeO_2 contact even when Pt/Al_2O_3 is physically mixed with CeO_2. Further evidence for the role of Pt–CeO_2 contact is provided by the decrease in the CO_2/CH_4 product ratio when the Pt particle size is increased. This indicates that the selectivity for production of CO_2 during methanation on CeO_2-containing Pt catalysts is influenced by metal–oxide interfacial area. The selectivity to formation of CO_2 during CO hydrogenation was also used to quantify Pt–CeO_2 contact in model automotive catalysts. It was found that the enhanced methanation activity of Pt/CeO_2 skews the CO_2/CH_4 ratio, decreasing the precision of this method for measuring the fraction of Pt in contact with CeO_2 in CeO_2–Al_2O_3 catalysts.

ACKNOWLEDGMENTS

This work was supported by a grant from the American Chemical Society, Petroleum Research Fund. Partial support from the Allied Signal Engineering Materials Research Center is also acknowledged. Transmission electron microscopy was performed at the Microbeam Analysis Facility at the University of New Mexico.

REFERENCES

1. Loof, P., Kasemo, B., and Keck, K. E., *J. Catal.* **118,** 339 (1989).
2. Harrison, B., Diwell, A. F., and Hallett, C., *Platinum Met. Rev.* **32,** 73 (1988).
3. Murrell, L. L., Tauster, S. J., and Anderson, D. R., presented at the 10th North American Catalysis Society Meeting, Lexington, KY, 1991.
4. Kalakkad, D., and Datye, A. K., presented at the 14th Organic Reactions Catalysis Meeting, Albuquerque, NM, 1992.
5. Blankenburg, K., and Datye, A. K., *J. Catal.* **128,** 186 (1991).
6. Tauster, S. J., Fung, S. C., and Garten, R. L., *J. Am. Chem. Soc.* **100** (1), 170 (1978).
7. Yao, M. H., Smith, D. J., Kalakkad, D. S., and Datye, A. K., *Z. Phys. D* **26s,** S79 (1993).
8. Kalakkad, D. S., Master's Thesis, University of New Mexico, 1993.
9. Jin, T., Okuhara, T., Mains, G. J., and White, J. M., *J. Phys. Chem.* **91,** 3310 (1987).
10. Kalakkad, D. S., Datye, A. K., and Robota, H. J., *Appl. Catal. B* **1,** 191 (1992).
11. Kepinski, L., and Wolcryz, M., *Catal. Lett.* **14,** 329 (1992).
12. Nunan, J., and Robota, H. J., paper presented at the 10th North American Catalysis Society, Pittsburgh, PA, May 1993.
13. Rodríguez-Reinosos, F., Rodríguez-Ramos, I., Moreno-Castilla, C., Guerrero-Ruiz, A., and López-Gónzalez, J. D., *J. Catal.* **107,** 1 (1987).
14. Nunan, J. G., Robota, H. J., Cohn, M. J., and Bradley, S. A., *J. Catal.* **133,** 309 (1992).
15. Yao, H. C., and Yao, Yu F., *J. Catal.* **86,** 254 (1984).